

---

---

# Investigation of Noise Reduction in Vehicle Floor Panels Through Damping Pads: Implications for Human Hearing and Noise Exposure Levels

**Shahin HASANI**

*Iran University of Science and Technology, Tehran, Iran, shaunhase1992@gmail.com*

**Mojtaba AGHAMIRZAEI**

*R&D Center, Irankhodro Company, Tehran, Iran, m.ghamirzai@mail.ikco.ir*

**Javad MARZBANRAD \***

*Iran University of Science and Technology, Tehran, Iran, marzban@iust.ac.ir*

\* Author to whom correspondence should be addressed

*Abstract:* - High noise exposure levels and prolonged noise exposure have negative physical and mental impacts. This study provides a review of the health effects associated with noise exposure, the regulations and laws that govern permissible noise levels, and a novel approach to assessing the human response to noise exposure. Subsequently, the issue of vehicle interior noise, which significantly contributes to daily noise exposure, was tackled by focusing on reducing the noise levels caused by floor panels by employing damping materials. While the most effective approach to noise reduction is to install damping material on all floor panels, choosing to cover only specific areas exhibiting the most intense vibrations is more cost- and time-efficient and averts the complications that may arise from the extra mass of damping materials. To achieve this, a finite element model of the front, center, and rear floors and all adjacent panels was created, and the critical areas for damping material placement were determined by performing a frequency response analysis (FRA) and studying the dynamic behavior of the FE model via MSC Nastran software. Installing damping pads using this optimal method only increased the mass of the floor by 2.6%. The noise reduction by damping pads becomes evident by a reduction of up to 4 percent in average A-weighted noise values at three critical points with and without said pads. Furthermore, in order to examine the impact of damping pads on human noise exposure, the A-weighted average noise levels were computed and compared prior to and following the installation of damping pads. The positive impact of noise reduction by damping pads on noise exposure and, as a result, human well-being is illustrated and emphasized by the A-weighted average noise level's ( $L_{eqA}$ ) reduction of up to more than 3 percent.

*Keywords:* - Noise, Health, NVH, FEM, Damping material, Floor panel.

---

## 1. INTRODUCTION

Nowadays, noise pollution is regarded as a serious problem that harms the health and well-being of the general population. It can decrease life span and quality while causing the costs of healthcare, the rate of specific diseases, and even mortality rates to increase [1, 2].

Since the vehicle is an environment in which people spend a portion of their daily lives based on their occupation and lifestyle, the vehicle's interior noise can be a significant contributor to noise exposure and its associated risks and problems. Furthermore, the subjective experience of automotive driving is primarily influenced by noise, and excessive interior noise has a significant impact on ride comfort and NVH performance.

Thus, interior sound quality (SQ) has become an important factor for automakers and customers [3, 4].

Frequency-wise, the internal noise can be separated into three parts: high-frequency airborne noise at frequencies over 500 Hz created by the vehicle's systems and aerodynamic disturbances that transfer through the cabin and are audible to the passengers; mid- and low-frequency structural sounds below 500 Hz caused by the transmission of mechanical inputs (engine, trains) through the car body frame [5, 6]. The use of sound insulation and absorption materials in a vehicle can be an effective method to minimize the level of high-frequency airborne noise [6].

In recent years, active noise control (ANC) approaches have emerged as a significant area of research interest due to their viability and efficiency in controlling low-frequency noise. Active noise control, commonly known as ANC, is based on the superposition of waves in an inverse phase, and its implementation may be separated into two different

---

---

categories: active sound control (ASC) and active vibration control (AVC) [7].

In the modern automotive industry, two primary methods are widely employed to reduce mid-frequency (20–500 Hz) noise: The first method involves filtering mechanical inputs in proximity to sources of vibration. For instance, installing engine mounts can reduce the transfer of energy between the vehicle's engine and body frame. The second method involves utilizing passive damping systems, typically located on the noise-radiating panels [8].

Typically, passive damping systems consist of patches that contain a viscoelastic layer. These systems can convert vibratory energy into shearing deformation of the viscoelastic layer [9]. To intelligently design passive damping systems that are lightweight, affordable, durable, efficient, and robust, it is necessary to have accurate Finite Element (FE) models that can predict the response of damping pads containing viscoelastic layers in terms of frequency.

Additionally, computer-aided design typically takes a shorter amount of time. To rapidly evaluate a large number of potential technical solutions during the design phase, it is necessary to generate models at a low cost and find solutions quickly. There are different approaches based on linear FE analysis to model damping materials. These methods are generally categorized as follows [10, 11]:

The first category, named the simple mass method, is the most commonly used approach. Based on this method, when defining the finite element of the part, the added mass of the damping material is considered, but its viscoelastic nature is largely ignored. Modeling for this method is relatively simple; however, it doesn't consider effects such as changes in stiffness and damping that are associated with the viscoelastic properties of the damping materials [12].

The second category, known as the explicit modeling method, on the other hand, requires a more complicated modeling process since it accounts for said potential effects [13].

In this study, the viscoelastic layer is modeled as a solid element, and its associated material properties are properly introduced into the Nastran software [14].

The novelty of the current research work is highlighted through the following key contributions:

1. Optimization of Damping Pad Placement: The study employs finite element method (FEM) analysis to identify optimal locations for installing damping pads by targeting areas with the highest noise levels, rather than covering the entire surface of the floor panels. This approach effectively mitigates noise while minimizing the additional mass added to the vehicle floor.

2. Application of A-Weighting for Human Hearing Analysis: The research incorporates A-weighting to assess the impact of noise reduction on human hearing, ensuring that the evaluation aligns with the frequency sensitivity of the human auditory system.

3. Assessing the Health effects of Noise Reduction: By calculating and comparing A-weighted average noise levels ( $L_{eqA}$ ), the study evaluates the effectiveness of noise reduction measures in lowering noise exposure levels and their subsequent implications for human health.

## 2. NOISE EFFECT ON HEALTH AND WELL-BEING

### 2.1. Health effects of noise exposure

Multiple studies indicate that exposure to environmental noise is detrimental to physiological and psychological health [1, 2]. The perception of noise appears to be subjective and dependent on some variables, including time, place, the people themselves, and how they interact with their surroundings. In real-world situations, the amount of noise exposure and the type of noise source vary between social groups. For instance, manual laborers are more subject to and affected by industrial noise. The psychological response to noise exposure can vary depending on the source of the noise, as well as between men and women [15].

Based on the functions regarding noise exposure and response provided by the World Health Organization (WHO), noise annoyance, sleep disturbance, and ischemic heart disease can be regarded as the primary effects of noise exposure in populations. Noise annoyance is a quantifiable indicator of the disruptive impact that noise exposure can have on various facets of daily life, including communication, concentration, and emotional control and regulation [2].

Exposure to nighttime noise can harm sleep patterns and also have daytime consequences, such as affecting cognitive ability, memory performance, and overall quality of life.

In addition, if sleep is disrupted due to noise exposure, this can result in negative cardio-metabolic effects such as high blood pressure, elevated levels of stress hormones, abnormal blood sugar levels, issues with blood sugar stability, and an altered appetite.

Noise exposure during the daytime contributes to a variety of health conditions, including diseases related to chemical processes that affect the cardiovascular system (e.g., ischemic heart disease (IHD), stroke, and diabetes), although the majority of studies point to road traffic noise sources as the

---

---

primary contributors to the aforementioned conditions [1].

According to some research, the primary cause of noise-related health problems in European countries is noise from road traffic, and since the levels of noise exposure for more than one-fifth of the population of Europe are higher than recommended, it is considered the second most significant public health risk after air pollution [1, 2].

## 2.2. Standards and regulations

The Occupational Safety and Health Administration (OSHA) has issued some guidelines regarding occupational noise exposure and procedures that must be implemented to address and combat the issue [16].

According to OSHA, employers are required to provide hearing conservation programs for their employees if the noise exposure levels are at or above 85 dB for 8 hours of work or if the time-weighted average of noise exposure levels during the period of time is at or above 85 dB. In addition, the maximum permissible noise exposure level, or the time-weighted average for 8 hours of work, is set at 90 dB. Increasing the level of noise exposure by 5 dB halves the duration of exposure. For example, if noise levels increase to 95 dB, the permissible exposure time is reduced to four hours.

Since employees do not always have access to measuring devices or data providing information about noise levels in the workplace, OSHA has established signs and methods to alert them when noise levels exceed critical levels. For instance, if a worker must raise their voice to be heard by a coworker who is an arm's length away (3 feet), this may be an indication that the noise level in the workplace exceeds 85 decibels.

Some indicators suggest workplace noise is a problem. Among these indicators are:

(1) After departing the workplace, the ears are ringing and humming.

(2) Experiencing temporary hearing loss

Chapter 11 of the World Health Organization's (WHO) health and environment guidelines discusses environmental noise and the permissible noise levels for various noise sources and times of day. It defines some variables as noise measurement indicators. These indicators are as follows [17]:

- a)  $L_{den}$  it is defined as the annual average noise levels over all days, evenings, and nights. It is measured in decibels.
- b)  $L_{night}$  is the continuous sound pressure level (in decibels), with nighttime serving as the reference time interval.

- c)  $L_{Aeq,T}$  is the A-weighted average noise level over a period of time (T) beginning at  $t_1$  and ending at  $t_2$ . It is measured in decibels at a point in space.

A-weighting is the standard weighting for audible frequencies. The frequencies between 20 Hz and 20 kHz are weighted during implementation. This weighting is intended to reflect the aural response of humans to noise. This is the reason why the weighted range of frequencies corresponds to the human ear's hearing range.

The majority of the time, indicators  $L_{den}$  and  $L_{night}$  are used to measure noise level and noise exposure. While  $L_{Aeq,T}$  is used to measure noise exposure for leisure noise sources.

The following are the recommended noise levels for typical noise exposure and various noise sources:

For sources of road traffic noise,  $L_{den}$  should be less than 53 dB.

- d)  $L_{den}$  should be below 54 dB for railway noise.
- e)  $L_{den}$  should be lower than 45 dB for aircraft noise.
- f) The value of  $L_{den}$  should be less than 45 dB for noise from wind turbines.
- g) The average annual noise exposure from all leisure noise sources (measured daily,  $L_{Aeq,24h}$ ) should not exceed 70 dB.
- h) The weekly average noise exposure from leisure noise sources (such as personal audio players) should be less than or equal to 80 dB.
- i) The average exposure to leisure noise sources for brief durations (e.g.,  $L_{Aeq,15min}$ ) should not exceed 100 decibels.

The following are the recommended noise levels for nighttime exposure:

- a) For road traffic noise:  $L_{night} < 45 \text{ dB}$
- b) For Railway noise:  $L_{night} < 44 \text{ dB}$
- c) For aircraft noise:  $L_{night} < 40 \text{ dB}$

## 2.3. A novel approach for assessing noise exposure

The current comprehension of noise exposure and its health effects is limited. The prevalent assumption is that the effects of noise exposure are related to it in a stationary manner. Additionally, when the objective is to gain a comprehension of the noise exposure, the response, and its effects, only one characteristic of sound, namely the sound pressure level, is investigated.

To better comprehend the complex nature of noise exposure, sound increment is defined as a new sound characteristic. It intends to demonstrate the abrupt increase in sound pressure levels. Along with sound

pressure level, this variable can be used to assess various aspects of noise exposure in real-world situations [15].

In the field of Ecological Momentary Assessment (EMA), which is the examination of daily human behavior using frequently collected environmental data, the A-weighted average noise level ( $L_T$ ) is an invaluable resource. It is computed with the following equation [15]:

$$L_T = 10 \times \log\left(\frac{1}{|T|} \times \sum_{t=t_{min}}^{t_{max}} 10^{0.1 \times L_t}\right) \quad (1)$$

In which  $L_t$  is the frequently measured, A-weighted noise level at time  $t$  (in the present study, it is measured every 30 seconds), and  $|T|$  is the number of frequently recorded data over the time period  $T$ , which is set to 5 minutes.

The sound increment denotes the average increase in sound pressure level over a brief period of time,  $T$ . First, the transient sound increment for time  $t$  within the time interval  $T$  is defined. It is defined as the difference between  $L_t$  at time  $t$  and  $L_{T'}$  over the 5 minutes  $T'$  preceding time  $t$ . It is defined by Equation (2):

$$I_t = 10 \times \log(10^{0.1 \times L_t} - 10^{0.1 \times L_{T'}}) \quad (2)$$

For the time period  $T$ , the average sound increment,  $I_T$ , can be defined. Only positive values of the transitory sound increment are examined because it is assumed that only a rise in the sound pressure level leads to noise annoyance.  $I_T$  can be derived using Equation (3):

$$I_T = 10 \times \log\left(\frac{1}{|T, I_t > 0|} \times \sum_{t=t_{min}, I_t > 0}^{t_{max}} 10^{0.1 \times I_t}\right) \quad (3)$$

where  $|T, I_t > 0|$  is the number of times  $I_t$  has taken on a positive value during the time interval  $T$ .

This new characteristic of sound can improve the evaluation of noise exposure and provide new ways to correlate noise exposure with its adverse health effects.

Figure 1 depicts the sound level and the sound increment in terms of six distinct levels of noise annoyance, with 1 being the least annoying and 6 being the most. The boxes represent an overall description of sound characteristics according to the subjects who reported the corresponding level of noise annoyance, while the contours on either side represent a summary of the distribution of sound characteristics based on local statistics.

The line that connects the median of the characteristics of sound corresponding to each annoyance level indicates that for short-term noise exposure, both higher sound pressure levels and

larger sound increments contribute to an increase in noise annoyance and susceptibility.

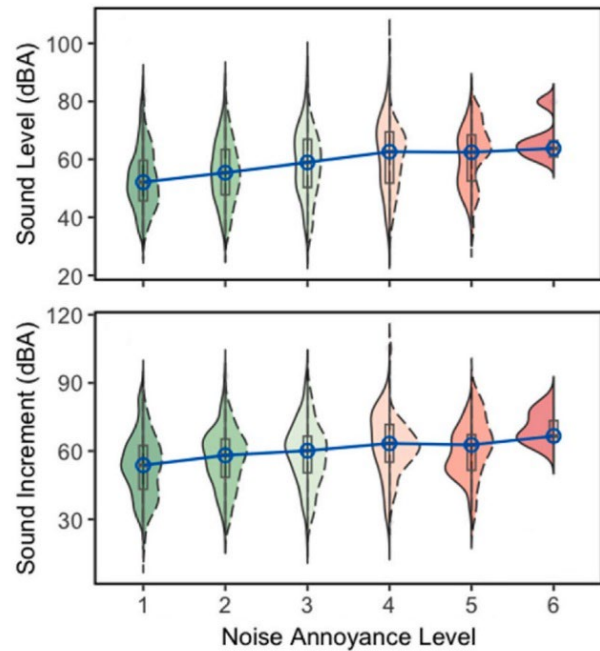


Figure 1. Sound level and sound increment for different noise annoyance levels [15]

There is a tri-variate relationship between noise aggravation, sound level, and sound increment, as shown in Figure 2. In other words, noise annoyance is dependent on both sound level and sound increment, and a change in either of these two sound characteristics can result in a change in noise annoyance levels.

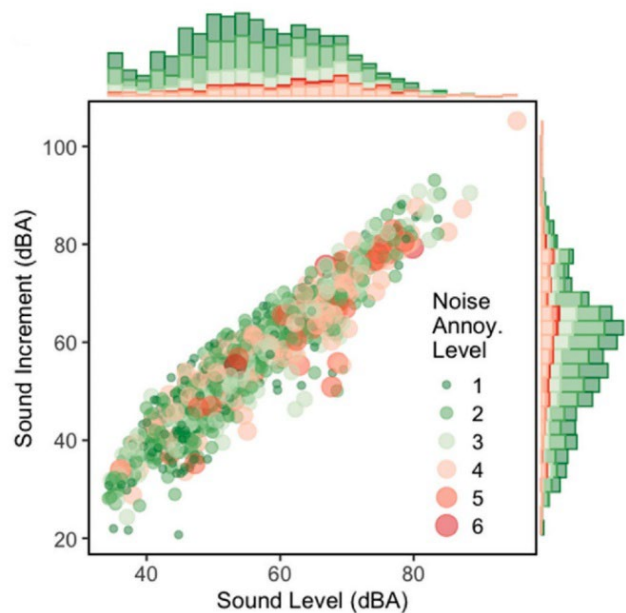


Figure 2. Tri-variate relationship between noise aggravation, sound level, and sound increment [15]

### 3. MODEL

To perform an FE analysis, MSC. Nastran 2010 is utilized. Samand BIW (body in white) panels were completely modeled and analyzed; however, just the underbody panels were requested in the resulting output as the main area of focus in this study. Solid elements with eight nodes and isotropic properties were used to model the viscoelastic layer. Panels were modeled by shell elements, and damping pads by solid elements.

Unit force excitation over the 0–500 Hz range was applied to the engine center of gravity. This excitation is transferred to the body through engine mounts modeled by springs. Vehicle suspensions were modeled by springs, and the ground nodes were constrained.

#### 3.1. Material modeling

The material properties of viscoelastic damping material consist of shear modulus and loss factor, shown in Figure 3 and Figure 4, respectively. The structural damping of the element (GE) was assumed to be equal to the loss factor when defining the finite element model's material card. The material properties of the viscoelastic damping pads depend on frequency and temperature. The ambient temperature was assumed to be 20°C [9].

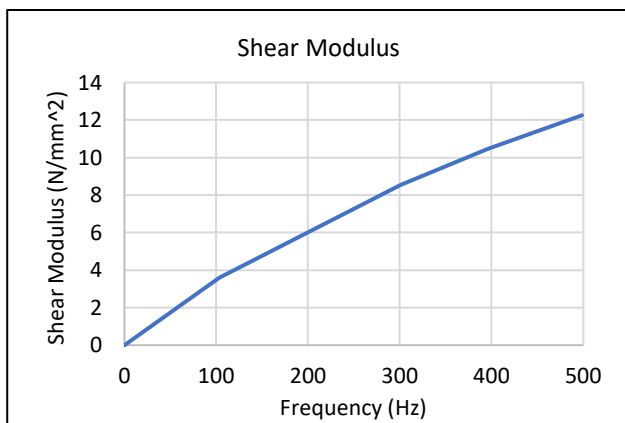


Figure 3. Shear modulus of the damping materials C-1002 (EAR Corporation)

Viscoelastic materials exhibit a dynamic behavior that is highly dependent on frequency, and their response under an excitation that is sinusoidal is steady, with the stress lagging behind the strain.

The stress of the viscoelastic material in a general 3D state is defined by a Poisson's ratio that has a real and constant value and a shear modulus that depends on the frequency and is described by a complex number.

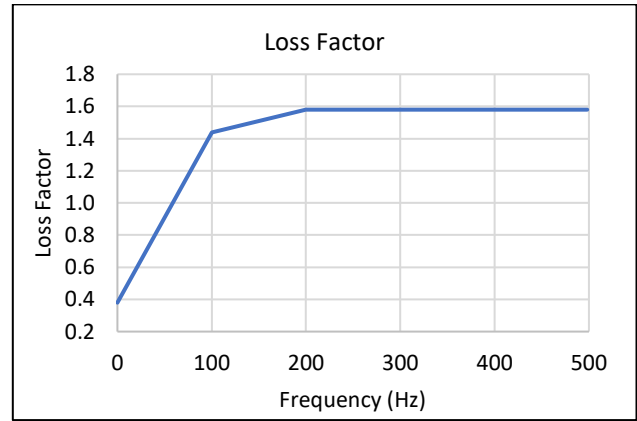


Figure 4. Loss factor of the damping materials C-1002 (EAR Corporation)

Using MSC. Nastran software, a scalar shear modulus that depends on the frequency and has a complex value, can be defined according to the following equation:

$$G(f) = G'(f) + iG''(f) \quad (4)$$

where  $G'(f)$  is the shear storage modulus,  $G''(f)$  is the shear loss modulus, and  $i$  denotes the imaginary unit.

The Shear loss factor is defined as the ratio of the shear loss modulus to the shear storage modulus and is calculated using Equation (5):

$$\eta = \frac{G''}{G'} \quad (5)$$

In direct frequency response analysis, the applied load in the frequency domain ( $F(f)$ ) is specified as a complex function in direct frequency response analysis, as illustrated by Equation (6):

$$F(f) = TR(f) + iTI(f) \quad (6)$$

where  $TR(f)$  denotes the real part and  $TI(f)$  denotes the imaginary part of  $F(f)$ , and  $i$  corresponds to the imaginary unit. Equations (7) and (8) can be employed to define the variables  $TR(f)$  and  $TI(f)$ , respectively:

$$TR(f) = \frac{1}{g_{REF}} \left[ \frac{G'(f)}{G_{REF}} - 1 \right] \quad (7)$$

$$TI(f) = \frac{1}{g_{REF}} \left[ \frac{G''(f)}{G_{REF}} - g \right] \quad (8)$$

where  $G_{REF}$  is the reference modulus,  $g_{REF}$  is the reference damping of the element, and  $g$  denotes the overall damping of the structure.

#### 3.2. Analysis method

As previously noted, the properties of the viscoelastic material depend on the frequency. And since properties that depend on the frequency can't be utilized in the modal frequency response solution, a

direct frequency response solution, including 200 modes with frequencies ranging between 0 and 500 Hz and considering a unit force excitation, was performed.

In the first step, the model was run without any damping pads using the direct frequency response method. Reviewing the results in the underbody area, about twenty-one points that had the highest vibration were selected as areas of focus. In the second step, viscoelastic damping pads were modeled by placing solid elements on top of the areas selected in the first step, and again, the FE model was run using the same method. Figure 5 shows the damping treatment areas.

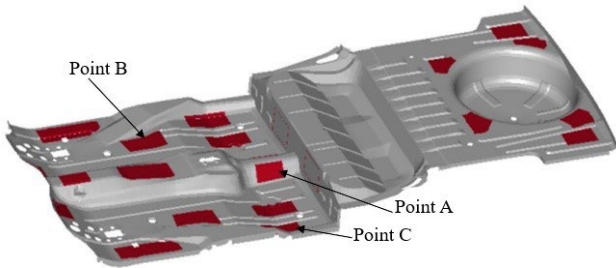


Figure 5. Underbody panels and damping area

#### 4. RESULT AND DISCUSSION

To analyze and illustrate the impact of damping pads, a comparison was conducted on the velocity amplitudes at Points A, B, and C (illustrated in Figure 5) in the frequency domain. Following this, the corresponding values of A-weighted noise levels in dBA were computed and compared using a reference velocity value ( $v_{ref} = 10^{-6} \text{ mm/s}$ ) and the A-weighting curve. The utilization of A-weighting was justified on the grounds that it accurately represents the response of the human ear to noise [18].

To evaluate the effect of noise reduction on noise exposure levels and their subsequent implications for human health, the A-weighted average noise levels were computed and compared between padded and unpadded conditions at each point. The inverse fast Fourier transform (IFFT) was implemented in MATLAB software to transform the noise data from the frequency domain to the time domain. 401 equally spaced frequency points were defined, with the interval between each consecutive frequency point set to exactly 1 Hz. Considering that the minimum and maximum frequencies ( $f_{min}, f_{max}$ ) is 100 and 500 Hz, respectively, the frequency resolution ( $\Delta f$ ) can be calculated using Equation (9):

$$\Delta f = \frac{f_{max} - f_{min}}{N - 1} = \frac{400}{400} = 1 \text{ (Hz)} \quad (9)$$

where  $N$  represents the total number of frequency points.

The total time duration ( $T$ ) corresponding to the frequency resolution was obtained using Equation (10):

$$T = \frac{1}{\Delta f} = 1 \text{ (s)} \quad (10)$$

The A-weighted average noise level was calculated using Equation (11):

$$L_{eqA} = 10 \log_{10} \left( \frac{1}{t_2 - t_1} \int_{t_1}^{t_2} |L(t)|^2 dt \right) \quad (11)$$

where  $L_{eqA}$  and  $L(t)$  are respectively the A-weighted average noise level and the instantaneous noise level in dBA, and  $t_1$  and  $t_2$  are the start and the end of the time, respectively. The parameters  $t_1$  and  $t_2$  were set as  $t_1 = 0$  and  $t_2 = 1$ .

Figure 6 depicts the frequency-dependent velocity at point A for two distinct modes: with and without damping pads.

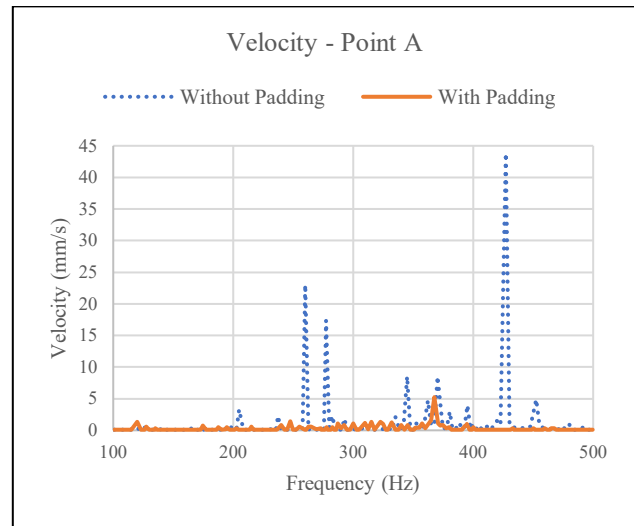


Figure 6. Velocity in terms of frequency at point A

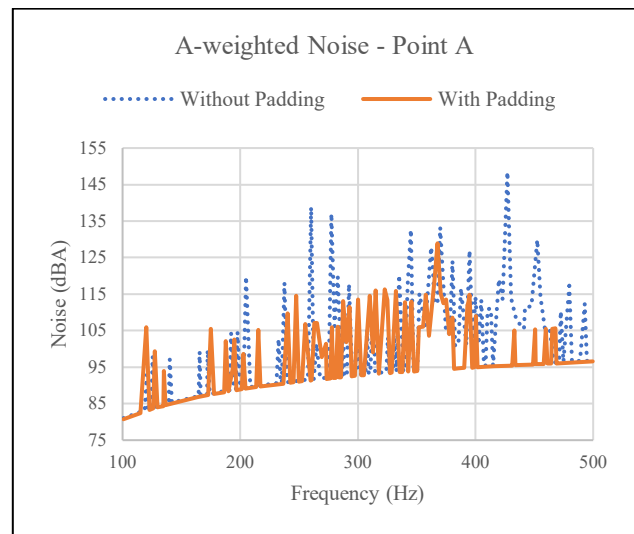


Figure 7. A-weighted noise in terms of frequency at point A

It is apparent from Figure 6 that the implementation of damping pads substantially influences the reduction of velocity amplitude, as the velocity curve becomes nearly horizontal after the damping pads are installed.

Figure 7 demonstrates the A-weighted noise levels for unpadding and padded situations at point A in terms of frequency.

By examining the A-weighted noise values presented in Figure 7, it is evident that the installation of damping pads effectively diminishes the magnitude and intensity of the peaks, particularly at higher frequencies.

The comparison of the frequency-based velocity at point B before and after the installation of damping pads is shown in Figure 8.

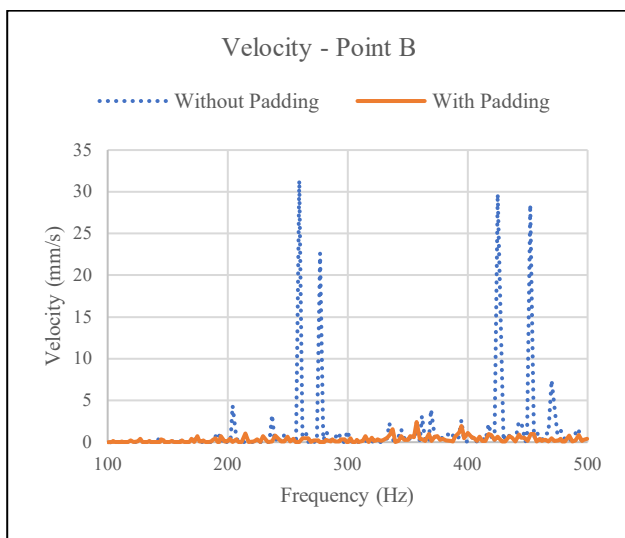


**Figure 8.** Velocity in terms of frequency at point B

Similar to the results at point A, damping pads effectively eliminate the velocity peaks at point B within the frequency range under consideration.

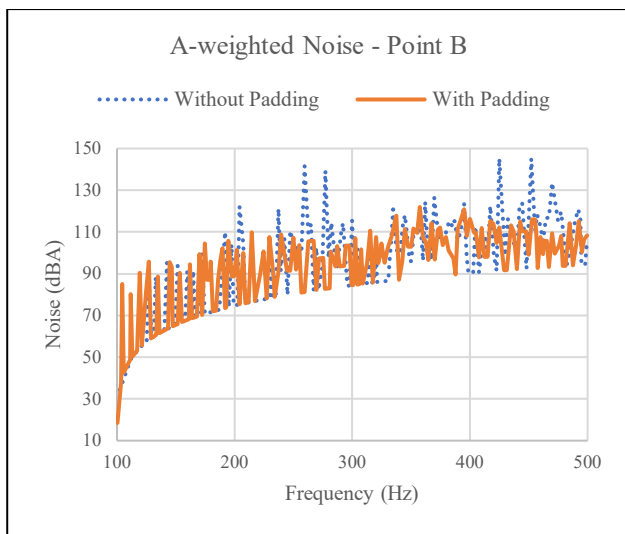


**Figure 9.** A-weighted noise in terms of frequency at point B

Figure 9 depicts the A-weighted noise level in terms of frequency at point B with and without the damping pads.

Evidently, the installation of damping pads at point B results in a decrease in peak intensity. However, it demonstrates a lesser degree of effectiveness compared to its performance at point A.

Figure 10 depicts the velocity at point C in terms of frequency for the unpadding and padded states

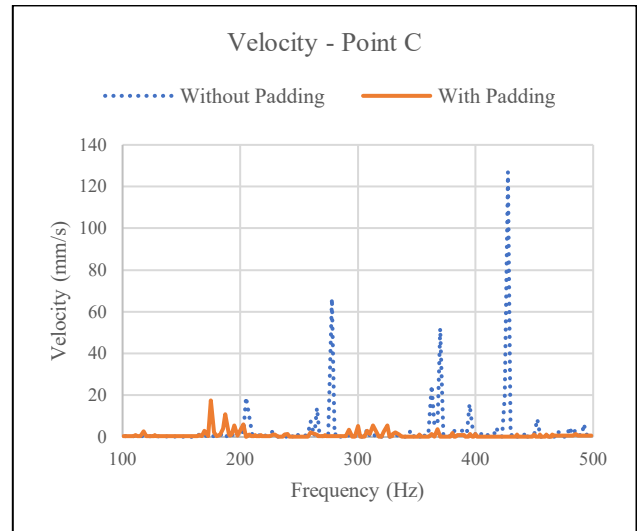


**Figure 10.** Velocity in terms of frequency at point C

When damping pads are present, the velocity curve at point C remains relatively flat across most frequencies. This indicates that the installation of damping pads eliminates the majority of the peaks in the velocity curve. However, there are some noticeable peaks in the padded mode, primarily found at low frequencies.

Figure 11 demonstrates the A-weighted noise level in terms of frequency when damping pads are not installed and when they are installed.

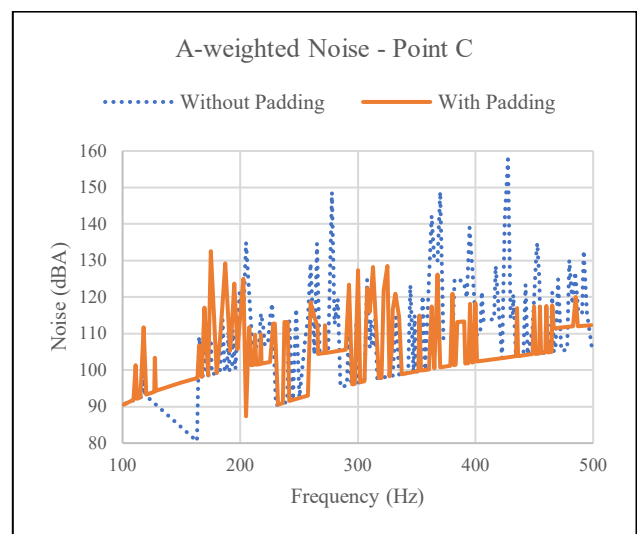


**Figure 11.** A-weighted SPL in terms of frequency at point C

Like the trend observed at points A and B, damping pads effectively mitigate the magnitude of peaks in the curve. One might argue that it exhibits superior performance at higher frequencies in comparison with pads located at point B.

Table 1 presents the average A-weighted noise values for points A, B, and C, as well as the percentage variation resulting from the presence of damping pads.

**Table 1.** Average A-weighted noise values

	Unpadded (dBA)	Padded (dBA)	Diff. (%)
A	101.94	99.13	2.75
B	97.50	94.42	3.15
C	111.80	107.51	3.83

The results indicate that damping pads consistently led to a decrease in average A-weighted noise values in all scenarios, with the most significant reduction observed at point C.

Table 2 displays the A-weighted average noise level ( $L_{eqA}$ ) values for points A, B, and C, along with the percentage variation caused by the presence of damping pads.

**Table 2.** A-weighted average noise level values

	Unpadded (dBA)	Padded (dBA)	Diff. (%)
A	11.0598	10.7018	3.34
B	10.8567	10.6358	2.07
C	11.7044	11.4454	2.26

The installation of damping pads decreases the average noise level, with the most notable decrease occurring at point A. This implies that it can effectively mitigate noise-related annoyance and health issues.

## 5. CONCLUSIONS

In this study, the effects of noise on health, laws and regulations regarding noise exposure levels, and a novel approach to better comprehending the response to noise exposure were discussed. Subsequently, vehicle interior noise as a prominent noise source in urban life was investigated, as was the reduction of floor panel noise as a significant contributor to vehicle interior noise. An FEM analysis was conducted to identify and select areas with the most intense vibrations. In selected areas, viscoelastic pads were used. These pads were modeled as solid

elements with eight nodes. To model viscoelastic materials in the MSc. Nastran, specific input data, including the loss factor and frequency-dependent shear modulus, are required. In this study, a direct frequency response solution was employed because the modal frequency response cannot be used to model viscoelastic materials, which have frequency-dependent properties. Based on the analysis, 21 points were chosen to be covered with damping pads.

Subsequently, three points were selected to illustrate the impact of installing damping pads: A, B, and C. A comparison was made between the A-weighted noise values, which represent the response of the human ear, before and after the installation of damping pads. The implementation of the damping pads effectively alleviated the pronounced noise peaks, and a 2 to 4 percent decline in the mean A-weighted noise levels was detected.

Furthermore, to examine the impact of damping on noise exposure and its subsequent effects on well-being, the A-weighted average noise level values were computed and compared using the inverse fast Fourier transform. A decrease ranging from 2 to 4 percent was noted in that particular instance, providing further evidence for the beneficial impact that damping pads have on human health and well-being.

## ACKNOWLEDGEMENTS

The authors would like to acknowledge Iran Khodro Co. for their support of this study. In addition, the authors acknowledge Mr. M. Osanlou and Mr. M. Razavi for their helpful discussions on material property.

## REFERENCES

- [1] C. Jephcote, S.N. Clark, A.L. Hansell, N. Jones, Y. Chen, C. Blackmore, K. Eminson, M. Evans, X. Gong, K. Adams, Spatial assessment of the attributable burden of disease due to transportation noise in England, *Environment International*, 2023, 107966.
- [2] G.M. Aasvang, L. Stockfelt, M. Sørensen, A.W. Turunen, N. Roswall, T. Yli-Tuomi, M. Ögren, T. Lanki, J. Selander, N. Vincens, Burden of disease due to transportation noise in the Nordic countries, *Environmental Research* 231, 2023, 116077.
- [3] Z. Liu, X. Li, S. Du, W. Chen, J. Shao, Q. Zheng, Strategy and implementing techniques for the sound quality target of car interior noise during acceleration, *Applied Acoustics* 182, 2021, 108171.
- [4] Y. Wang, S. Zhang, H. Guo, X. Wang, C. Yang, N. Liu, Hybrid time-frequency algorithm for active sound quality control of vehicle interior noise based on stationary discrete wavelet transform, *Applied Acoustics* 171, 2021, 107561.
- [5] X. Wu, Y. Kong, S. Zuo, P. Liu, Research on multi-band structural noise reduction of vehicle body based on two-degree-of-freedom locally resonant phononic crystal, *Applied Acoustics* 179, 2021, 108073.

- 
- 
- [6] H.B. Huang, X.R. Huang, M.L. Yang, T.C. Lim, W.P. Ding, Identification of vehicle interior noise sources based on wavelet transform and partial coherence analysis, *Mechanical Systems and Signal Processing* 109, 2018, pp. 247-267.
- [7] Y. Wang, H. Guo, Y. Li, N. Liu, C. Yang, Active control for vehicle interior noise based on DWT-FxLMS algorithm using a piezoelectric feedback system, *Applied Acoustics* 167, 2020, 107409.
- [8] S. Stawicki, X. Bohineust, F. Dupuy, Dimensionnement des traitements amortissants de structures automobiles par application du calcul éléments finis en dynamique, *Papier SIA 93011*, 1993.
- [9] Y. Kiyota, M. Asai, H. Sugita, A. Akiyama, Low frequency noise reduction by improving sound insulation materials, *SAE Technical Paper*, 1995.
- [10] H. Bloemhof, Optimization of Damping Treatment in the Car Design Process Using Advanced Simulation Techniques, *SAE Transactions*, 1995, pp. 2124-2131.
- [11] E. Barkanov, Transient response analysis of structures made from viscoelastic materials, *International Journal for Numerical Methods in Engineering* 44(3), 1999, pp. 393-403.
- [12] A. Chen, Y. Qian, Simulating low frequency NVH of damped automotive body panels using frequency dependent properties, *SAE Transactions* 108, 1999, pp. 3043-3047.
- [13] E. Balmes, S. Germes, Tools for viscoelastic damping treatment design. application to an automotive floor panel, *ISMA Conference Proceedings*, 2002.
- [14] A. Chen, Modeling of treated body panel damping and stiffness, *Internal Status Report*, Ford Motor Company, 1997.
- [15] J. Cai, M.-P. Kwan, Z. Kan, J. Huang, Perceiving noise in daily life: How real-time sound characteristics affect personal momentary noise annoyance in various activity microenvironments and times of day, *Health & Place* 83, 2023, 103053.
- [16] Occupational Noise Exposure – Overview, in: O.S.a.H.A. (OSHA) (Ed.).
- [17] Compendium of WHO and other UN guidance on health and environment, Chapter 11: Environmental Noise, in: W.H.O. (WHO) (Ed.), 2022.
- [18] Wang, *Vehicle noise and vibration refinement*, Elsevier, 2010.